

Supporting information

Mechanism and spectrum of inhibition of a 4'-cyano modified nucleotide analog against diverse RNA polymerases of prototypic respiratory RNA viruses

Calvin J. Gordon¹, Simon M. Walker¹, Egor P. Tchesnokov¹, Dana Kocincova¹, Jared Pitts², Dustin S. Siegel², Jason K. Perry², Joy Y. Feng², John P. Bilello², and Matthias Götte^{1*}

¹Department of Medical Microbiology and Immunology, University of Alberta, Edmonton, Alberta, Canada.

²Gilead Sciences, Inc., Foster City, California, USA

* To whom correspondence should be addressed: Matthias Götte: Department of Medical Microbiology and Immunology, University of Alberta, Edmonton, Alberta, Canada, T6G 2E1; gotte@ualberta.ca; Tel.1(780) 492-2308.

Table S1. Selective incorporation of GS-443902, a 1'-cyano purine NTP analog, by selected RdRp enzymes

Table S2. Selective incorporation of GS-646939, a 4'-cyano purine NTP analog, by selected RdRp enzymes

Table S3. Inhibitory effect of the incorporated analog-monophosphate on incorporation of the subsequent nucleotide

Figure S1. Selective incorporation of GS-443902 and GS-646939 by EV-71 RdRp.

Figure S2. Competitive incorporation of GS-646939 versus GS-443902 by HRV-16 and EV-71 RdRp.

Figure S3. Models of ATP in its pre-incorporated state for LASV, FluB, and, h-mtRNAP

Figure S4. SARS-CoV-2 and MERS-CoV RdRp-catalyzed RNA synthesis and inhibition patterns following a single incorporation of ATP or GS-646939 as a function of nucleotide concentration

Figure S5. RSV or HMPV RdRp-catalyzed RNA synthesis and inhibition patterns following the incorporation of GS-646939 as a function of nucleotide concentration

Figure S6. HPIV-3 or PIV-5 RdRp-catalyzed RNA synthesis and inhibition patterns following the incorporation of ATP, GS-646939, or GS-443902

Figure S7. GS-646939 inhibits subsequent nucleotide incorporation catalyzed by HRV-16 RdRp in a manner resembling EFdA.

Figure S8. RNA synthesis catalyzed by EV-71 RdRp using a template with a single GS-443902 or GS-646939 residue in the template at position 11

Figure S9. RNA synthesis catalyzed by MERS-CoV and SARS-CoV-2 RdRp using a template with a single GS-646939 residue embedded at position 11

Table S1: Selective incorporation of GS-443902, a 1'-cyano purine NTP analog, by selected RdRp enzymes

RNA Sense	Family (-viridae)	Virus	ATP			GS-443902			
			V_{max}^a (product fraction)	K_m^b (μ M)	V_{max}/K_m	V_{max} (product fraction)	K_m (μ M)	V_{max}/K_m	Selectivity ^f (fold)
Positive ssRNA	Corona-	SARS-CoV-2							0.28¹
		P.R. ^c	0.75 ^d ± 0.019	0.03 ± 0.003	25	0.74 ± 0.023	0.0089 ± 0.0020	83	
		SARS-CoV							0.32¹
		P.R.	0.73 ± 0.017	0.03 ± 0.003	24	0.70 ± 0.015	0.010 ± 0.0008	70	
	Picorna-	MERS-CoV							0.35¹
		P.R.	0.47 ± 0.011	0.017 ± 0.019	28	0.50 ± 0.012	0.0063 ± 0.0006	79	
		HRV-16							1.03
		0.90 ± 0.017	4.52 ± 0.31	0.20	0.96 ± 0.015	4.96 ± 0.27	0.19		
	EV-71							0.93	
		0.96 ± 0.021	0.96 ± 0.066	1.0	0.93 ± 0.027	0.86 ± 0.081	1.08		
Nonsegmented negative ssRNA	Pneumo-	RSV							2.73²
		P.R.	0.76 ± 0.022	0.17 ± 0.023	4.5	0.82 ± 0.027	0.50 ± 0.089	1.6	
		HMPV							6.71
			0.60 ± 0.024	6.40 ± 0.98	0.094	0.57 ± 0.045	42.19 ± 7.79	0.014	
	Paramyxo-	HPIV-3							7.20
				0.63 ± 0.025	0.061 ± 0.015	10.3	0.63 ± 0.010	0.44 ± 0.040	1.43
PIV-5								8.31	
		0.74 ± 0.026	1.5 ± 0.25	0.49	0.77 ± 0.042	13 ± 2.3	0.059		
Segmented Negative ssRNA	Orthomyxo-	FluB							68¹
		P.R.	0.73 ± 0.014	0.23 ± 0.020	3.2	0.45 ± 0.0064	9.7 ± 0.42	0.046	
	Arena-	LASV							20¹
		P.R.	0.57 ± 0.032	0.11 ± 0.020	5.2	0.35 ± 0.016	1.3 ± 0.18	0.27	
Human DNA-dependent RNA polymerase		h-mtRNAP							503²
		P.R.	0.98 ± 0.018	0.050 ± 0.0037	19.6	0.81 ± 0.013	21 ± 0.096	0.039	

^a V_{max} is a Michaelis–Menten parameter reflecting the maximal velocity of nucleotide incorporation.

^b K_m is a Michaelis–Menten parameter reflecting the concentration of the nucleotide substrate at which the velocity of nucleotide incorporation is half of V_{max}

^c Previously reported

^d All reported values have been calculated based on an 8–data point experiment repeated at least 3 times (n=3).

^e Standard error associated with the fit.

^f Selectivity of a viral RNA polymerase for a nucleotide substrate analog is calculated as the ratio of the V_{max}/K_m values for ATP and GS-443902 analog, respectively.

¹ Data from Gordon et al. (1)

² Data from Tchesnokov et al. (2)

Table S2: Selective incorporation of GS-646939, a 4'-cyano purine NTP analog, by selected RdRp enzymes

RNA Sense	Family (-viridae)	Virus	ATP			GS-443902			
			V_{max}^a (product fraction)	K_m^b (μ M)	V_{max}/K_m	V_{max} (product fraction)	K_m (μ M)	V_{max}/K_m	Selectivity ^f (fold)
Positive ssRNA	Corona-	SARS-CoV-2							1.37
			$0.84^c \pm^d 0.030$	0.057 ± 0.0078	14.74	0.88 ± 0.015	0.082 ± 0.0070	10.73	
		MERS-CoV							1.17
	Picorna-		0.84 ± 0.0090	0.032 ± 0.0014	26.25	0.90 ± 0.012	0.040 ± 0.0031	22.50	
		HRV-16							0.018
			0.90 ± 0.017	4.52 ± 0.31	0.20	0.80 ± 0.021	0.072 ± 0.0097	11.11	
Nonsegmented negative ssRNA	Pneumo-		0.96 ± 0.021	0.96 ± 0.066	1.0	0.93 ± 0.019	0.047 ± 0.0034	19.79	
		RSV							1.58
			0.61 ± 0.065	0.97 ± 0.36	0.63	0.80 ± 0.059	2.0 ± 0.52	0.40	
	Paramyxo-	HMPV							1.73
			0.39 ± 0.028	2.1 ± 0.41	0.19	0.53 ± 0.027	4.8 ± 0.99	0.11	
		HPIV-3							10.3
Segmented Negative ssRNA	Orthomyxo-		0.63 ± 0.025	0.061 ± 0.015	10.3	0.78 ± 0.012	0.78 ± 0.059	1.0	
		FluB							2288
	Arena-		0.68 ± 0.014	0.11 ± 0.0077	6.18	0.18 ± 0.0057	66 ± 4.1	0.0027	
LASV								225	
Human DNA-dependent RNA polymerase			0.80 ± 0.0037	0.39 ± 0.075	2.05	0.29 ± 0.091	31.95 ± 25.15	0.0091	
		h-mtRNAP							1538
			0.93 ± 0.026	0.096 ± 0.0091	9.69	0.67 ± 0.22	107 ± 60.71	0.0063	

^a V_{max} is a Michaelis–Menten parameter reflecting the maximal velocity of nucleotide incorporation.

^b K_m is a Michaelis–Menten parameter reflecting the concentration of the nucleotide substrate at which the velocity of nucleotide incorporation is half of V_{max} .

^c All reported values have been calculated based on an 8–data point experiment repeated at least 3 times (n=3).

^d Standard error associated with the fit.

^e Selectivity of a viral RNA polymerase for a nucleotide substrate analog is calculated as the ratio of the V_{max}/K_m values for ATP and GS-646939, respectively.

Table S3: Inhibitory effect of the incorporated analog-monophosphate on incorporation of the subsequent nucleotide

Virus	Primer 3'-end (base)	Substrate	V_{\max}^b (product fraction)	K_m^c (μM)	V_{\max}/K_m	Inhibition ^d (fold)
SARS-CoV-2	AMP	UTP	1.10 ± 0.043^f	0.009 ± 0.0015	122	Ref. ^g
	GS-646939 (MP ^a)		0.79 ± 0.036	16.42 ± 2.67	0.048	2542
	GS-443902 (MP)		1.13 ± 0.047	0.0082 ± 0.0013	138	0.88
MERS-CoV	AMP	UTP	1.03 ± 0.016	0.0016 ± 0.0001	644	Ref.
	GS-646939 (MP)		0.91 ± 0.10	24.68 ± 9.19	0.037	17,405
	GS-443902 (MP)		0.98 ± 0.018	0.0009 ± 0.0001	1089	0.59
HRV-16	AMP	UTP	0.76 ± 0.015	0.023 ± 0.002	33.04	Ref.
	GS-646939 (MP)		0.83 ± 0.012	18.88 ± 1.22	0.044	751
	GS-443902 (MP)		0.67 ± 0.015	0.057 ± 0.005	11.75	2.81
EV-71	AMP	UTP	0.65 ± 0.003	0.028 ± 0.0006	23.21	Ref.
	GS-646939 (MP)		0.81 ± 0.017	157 ± 10.25	0.005	4,642
	GS-443902 (MP)		0.48 ± 0.005	0.093 ± 0.003	5.16	4.50
RSV	AMP	UTP	0.70 ± 0.037	1.6 ± 0.41	0.44	Ref.
	GS-646939 (MP)		0.15 ± 0.0029	354 ± 16	0.00042	1,048
	GS-443902 (MP)					6.27¹
HMPV	AMP	UTP	0.48 ± 0.026	7.8 ± 2.2	0.062	Ref.
	GS-646939 (MP)		0.087 ± 0.030	732 ± 488	0.00012	517
	GS-443902 (MP)		0.28 ± 0.018	22 ± 6.2	0.013	4.77
HPIV-3	AMP	UTP	0.56 ± 0.0097	0.073 ± 0.0093	7.67	Ref.
	GS-646939 (MP)		0.61 ± 0.0099	268 ± 11	0.0023	3,334
	GS-443902 (MP)		0.58 ± 0.011	0.076 ± 0.011	7.63	1.01
PIV-5	AMP	UTP	0.51 ± 0.022	5.8 ± 1.3	0.088	Ref.
	GS-646939 (MP)		0.058 ± 0.080	2740 ± 4899	0.000021	4,190
	GS-443902 (MP)		0.48 ± 0.0089	2.2 ± 0.26	0.22	0.40

^a Denotes that the 3'-end of the primer is terminated by the monophosphate form of the respective nucleotide.

^b V_{\max} is a Michaelis–Menten parameter reflecting the maximal velocity of nucleotide incorporation.

^c K_m is a Michaelis–Menten parameter reflecting the concentration of the nucleotide substrate at which the velocity of nucleotide incorporation is half of V_{\max} .

^d Inhibition of subsequent nucleotide incorporation is calculated as the ratio of V_{\max}/K_m values for UTP determined on primers terminated with AMP, GS-646939, or GS-443902.

^e All reported values have been calculated based on an 8–data point experiment repeated at least 3 times (n=3).

^f Standard error associated with the fit.

^g Reference.

¹ Data from Tchesnokov et al. (2)

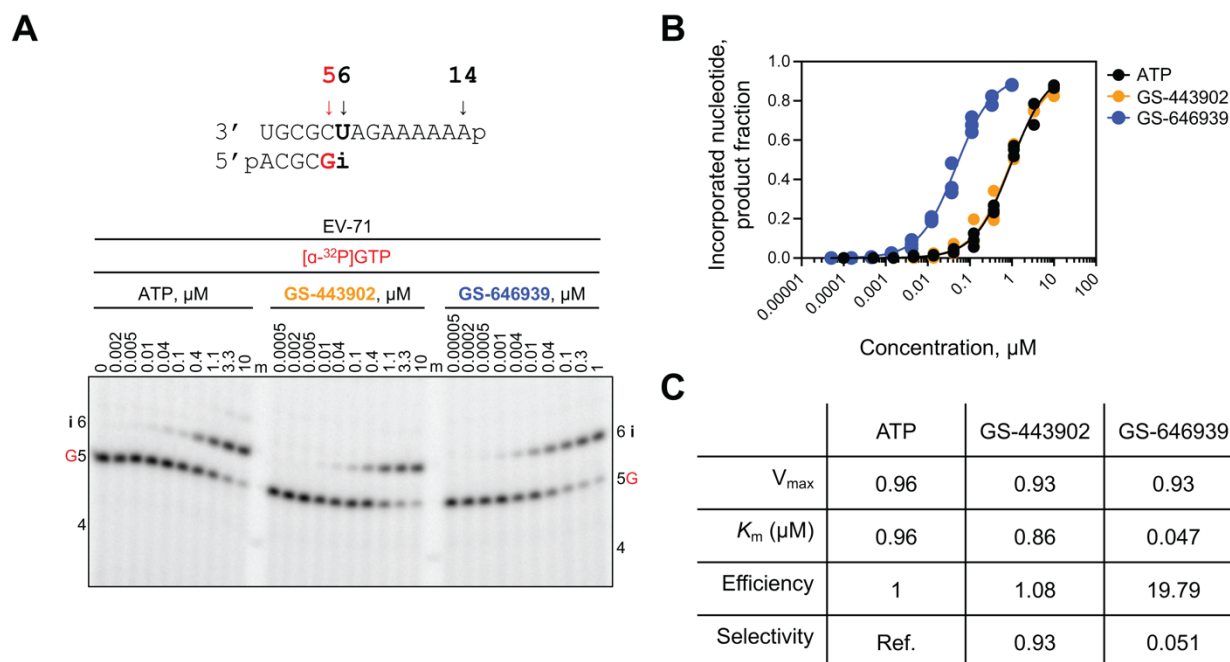


Figure S1. Selective incorporation of GS-443902 and GS-646939 by EV-71 RdRp. **A**, RNA primer/template substrate used in the RNA synthesis assays to test GS-443902 and GS-646939 as substrates for incorporation at position 6 (“i”) is shown above the gel. G indicates incorporation of the radiolabelled nucleotide opposite template position 5. NTP incorporation was monitored with purified EV-71 RdRp in the presence of [α -³²P]-GTP, RNA primer/template, MgCl₂ and increasing concentrations of ATP or the respective ATP analog substrate. Lane m illustrates the migration pattern of the radiolabelled 4 nucleotide-long primer. **B**, Graphical representation of the incorporation of ATP and ATP analogs shown in **A**, fitting the data points to the Michaelis-Menten function to determine V_{max} and K_m . Independent 8-data point experiments were performed at least three times ($n=3$), each replicate is plotted to represent the variation between experiments. **C**, Kinetic parameters and efficiency of ATP, GS-443902, and GS-646939 incorporation by EV-71 RdRp. Efficiency is determined as the quotient of V_{max} over K_m and selectivity as the quotient of natural ATP efficiency over the efficiency of the ATP analog.

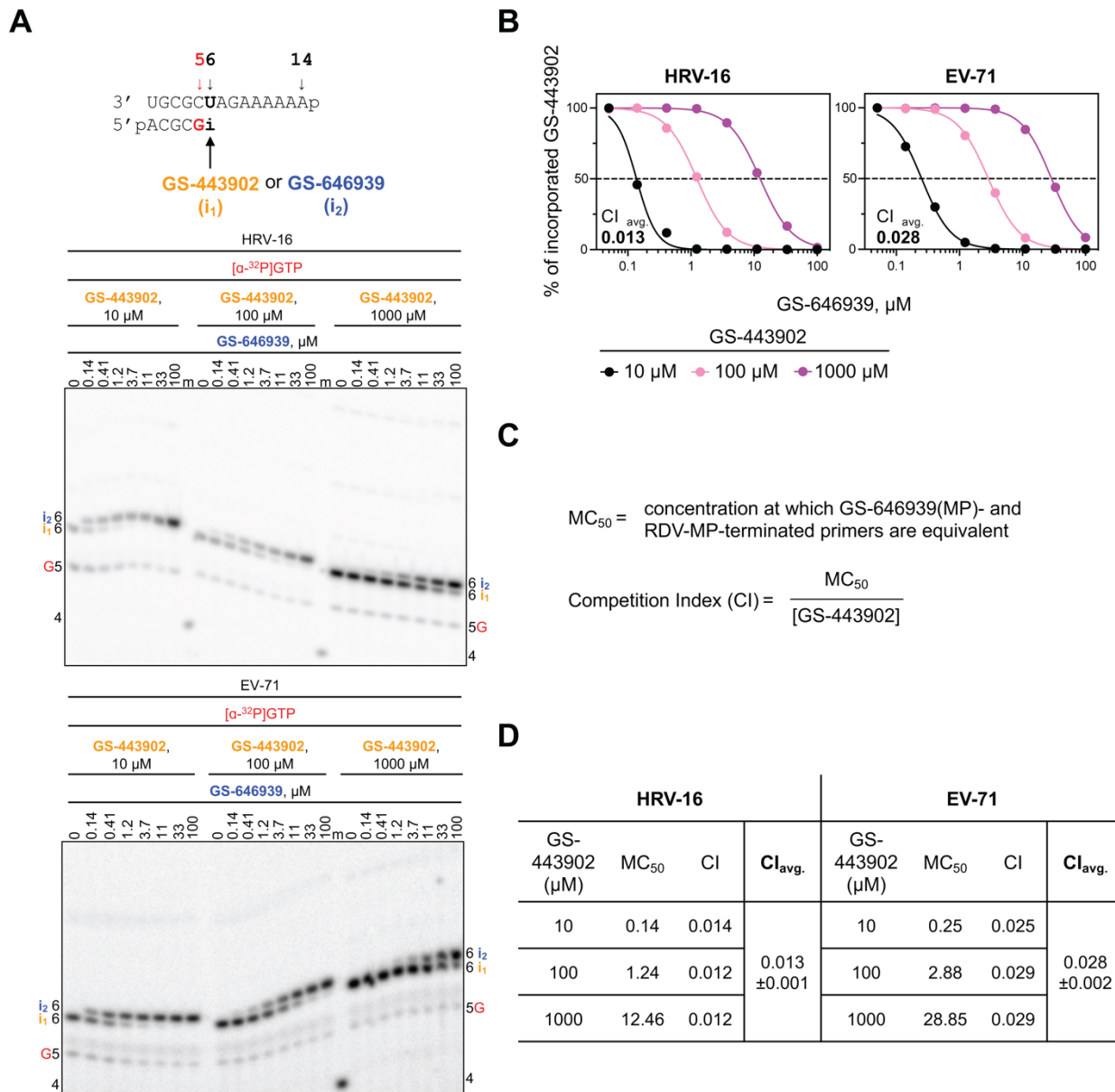


Figure S2. Competitive incorporation of GS-646939 versus GS-443902 by HRV-16 and EV-71 RdRp. **A**, RNA primer/template (top) supporting a single incorporation of GS-443902 (“i₁”) or GS-646939 (“i₂”) at position 6. G indicates incorporation of [α -³²P]-GTP at position 5. Migration pattern of RNA synthesis products catalyzed by HRV-16 (middle) and EV-71 RdRp (bottom). Product formation resulting in GS-443902- or GS-646939-terminated primers were compared across increasing GS-646939 concentrations at GS-443902 concentrations of 10, 100, and 1000 μM. A 5'-³²P-labeled 4-nt primer serves as a size marker. **B**, Graphical representation of GS-443902-terminated primers (%) at increasing GS-646939 concentrations as shown in **A**. **C**, The MC_{50} value is defined as the concentration at which GS-646939 outcompetes GS-443902 for incorporation at position 6. The competition index (CI) is the ratio of the MC_{50} value to the GS-443902 concentration present in the reaction. **D**, CI values determined for HRV-16 and EV-71 RdRp and the CI average (CI_{avg}) and standard deviation (\pm) across all GS-443902 concentrations.

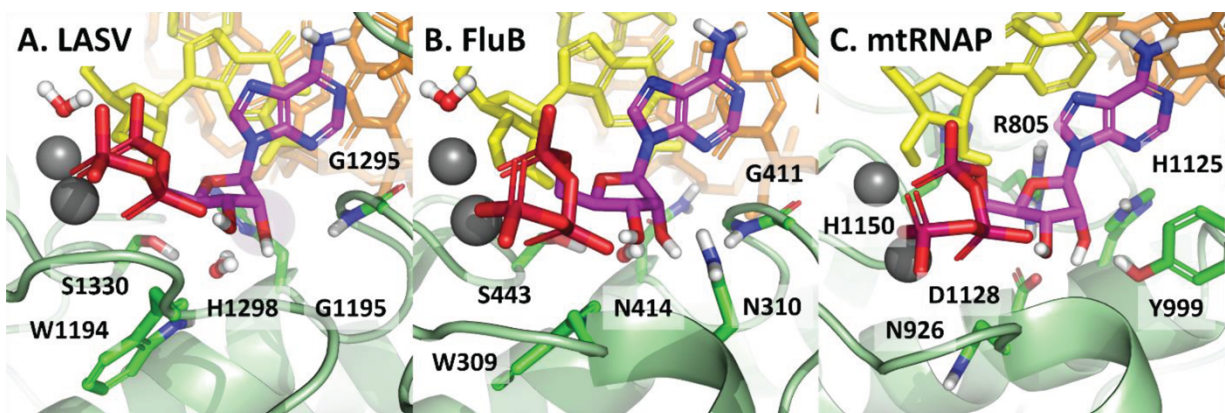


Figure S3. Models of ATP in its pre-incorporated state for *A*, LASV, *B*, FluB, and *C*, h-mtRNAP. The active sites of LASV and FluB are similar to RSV and PIV5, but differ significantly in the specific residues which recognize the 2'-OH and define the 4' pocket. In particular, a bridging water molecule is predicted to be a key element in the recognition of the 2'-OH. This is likely displaced by the 4'-cyano of GS-646939, compromising its affinity for these polymerases. The active site for h-mtRNAP is structurally very different from the viral polymerases. The 4'-cyano of GS-646939 appears to conflict with a salt bridge formed by Arg-805 and Asp-1128, which sit just below the ribose, making it a poor inhibitor.

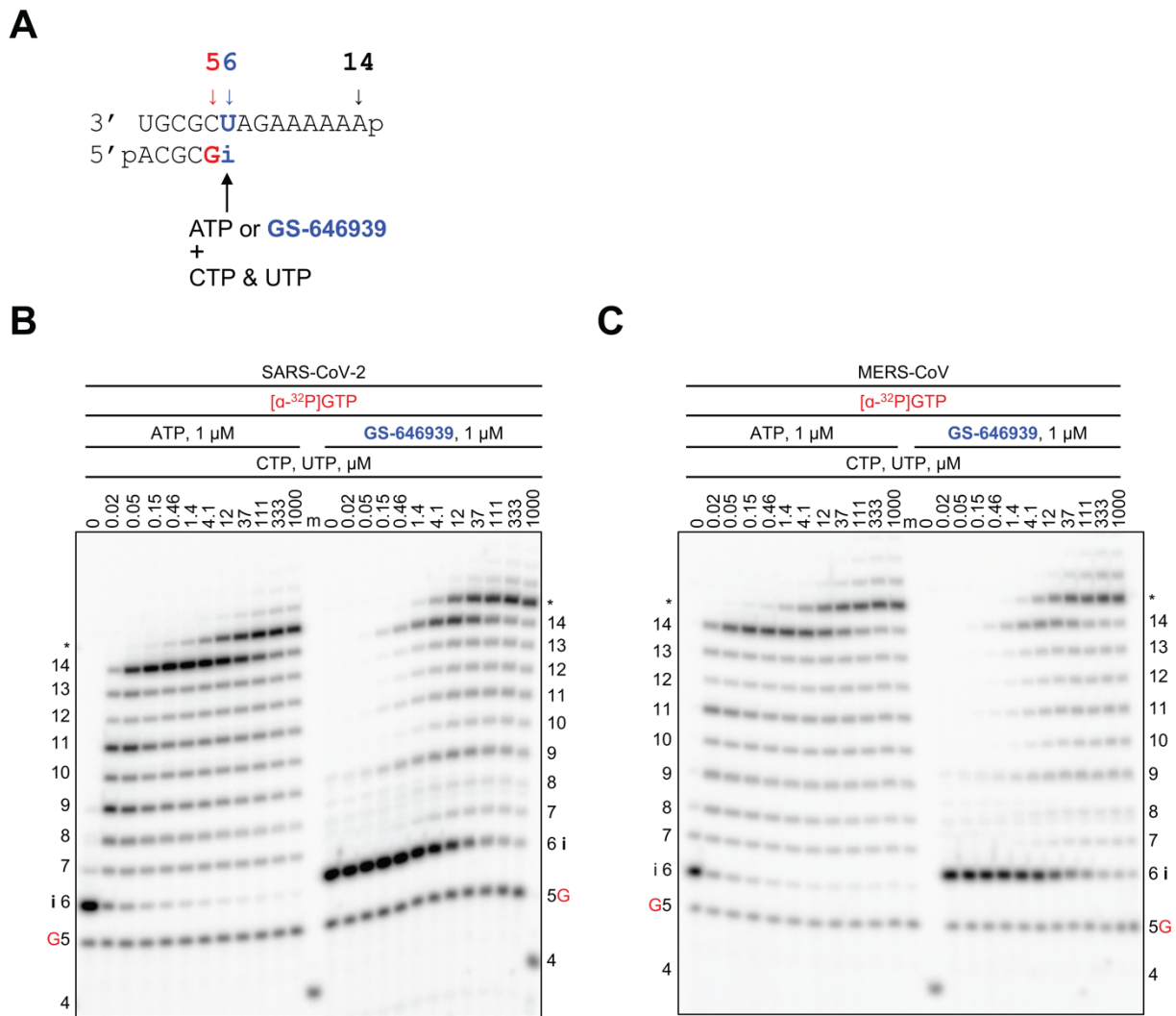


Figure S4. SARS-CoV-2 and MERS-CoV RdRp-catalyzed RNA synthesis and inhibition patterns following a single incorporation of ATP or GS-646939 as a function of nucleotide concentration. **A**, RNA primer/template supporting RNA synthesis and single incorporation of ATP or GS-646939 at position 6 (“i”). G indicates incorporation of [α - 32 P]-GTP at position 5. **B**, Migration pattern of RNA products resulting from SARS-CoV-2 RdRp catalyzed RNA extension of AMP (*left*) of GS-646939 (*right*) at increasing concentrations of CTP and UTP. A 5'- 32 P-labeled 4-nt primer serves as a size marker. Product formation at and beyond the asterisk indicate RNA products that are likely a result of sequence-dependent slippage events. **C**, Reactions with MERS-CoV RdRp, incomplete inhibition of RNA synthesis occurs at the site of GS-646939 incorporation, full template-length product is generated at elevated nucleotide concentrations.

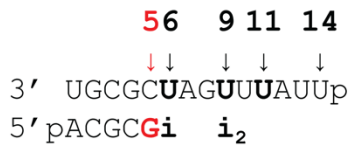
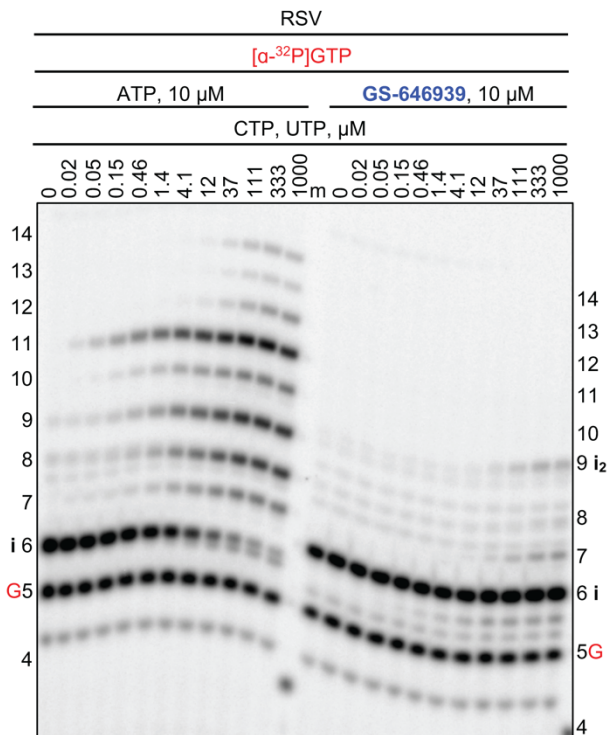
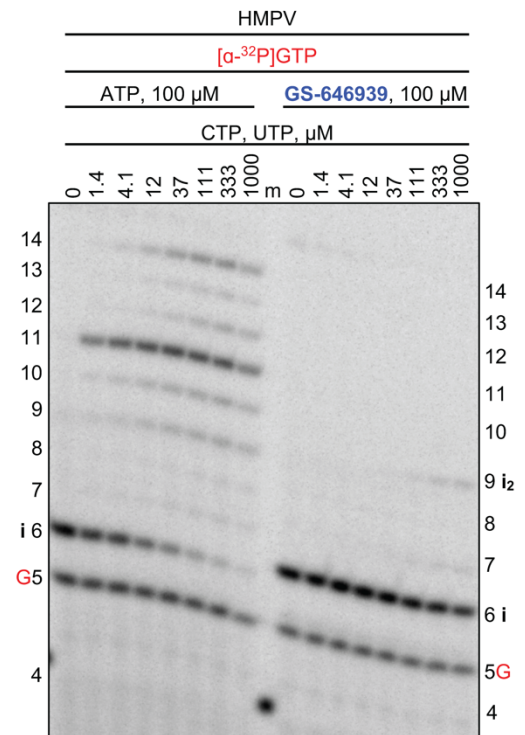
A**B****C**

Figure S5. RSV or HMPV RdRp-catalyzed RNA synthesis and inhibition patterns following the incorporation of GS-646939 as a function of nucleotide concentration. **A**, RNA primer/template supporting RNA synthesis and a first and second incorporation of ATP or GS-646939 by RSV and HMPV RdRp at position 6 (“i”) and 9 (“i₂”). G indicates incorporation of [α-³²P]-GTP at position 5. **B**, Migration pattern of RNA products resulting from RSV RdRp-catalyzed RNA extension of AMP (*left*) or GS-646939 (*right*) at increasing concentrations of CTP and UTP. A 5′-³²P-labeled 4-nt primer serves as a size marker. **C**, Migration patterns of RNA products catalyzed HMPV RdRp, RNA synthesis was monitored at increasing CTP and UTP concentrations when ATP (*left*) or GS-646939 (*right*) were incorporated at position 6. GS-646939-terminated primers fail to be extended.

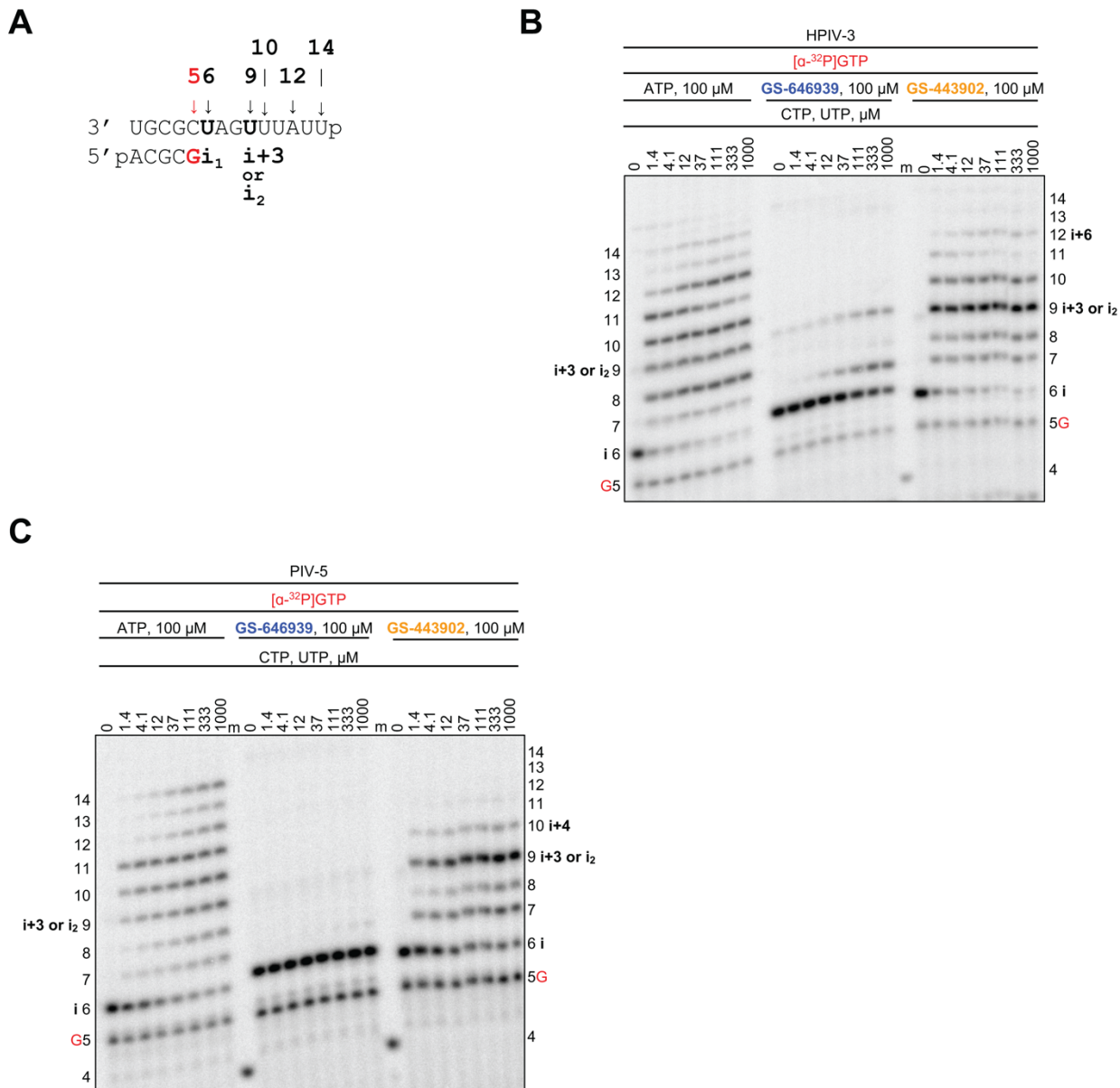


Figure S6. HPIV-3 or PIV-5 RdRp-catalyzed RNA synthesis and inhibition patterns following the incorporation of ATP, GS-646939, or GS-443902. **A**, RNA primer/template supporting RNA synthesis and a first and second incorporation of ATP or GS-646939 or GS-443902 at position 6 (“i₁”) and 9 (“i₂”). G indicates incorporation of [α -³²P]-GTP at position 5. **B**, Migration patterns of RNA products catalyzed HPIV-3 RdRp. RNA synthesis was monitored at increasing CTP and UTP concentrations when natural ATP (*left*), GS-646939 (*middle*), or GS-443902 (*right*) were incorporated at position 6. GS-646939 termination was nearly absolute, whereas RNA products can be observed up to position 12 following the incorporation of GS-443902. **C**, Migration patterns of RNA products catalyzed PIV-5 RdRp, RNA synthesis was monitored at increasing CTP and UTP concentrations when natural ATP (*left*), GS-646939 (*middle*), or GS-443902 (*right*) were incorporated at position 6. PIV-5 RdRp failed to catalyze RNA products beyond an incorporated GS-646939, while GS-443902 could be readily extended to position 9 (“i+3” or “i₂”).

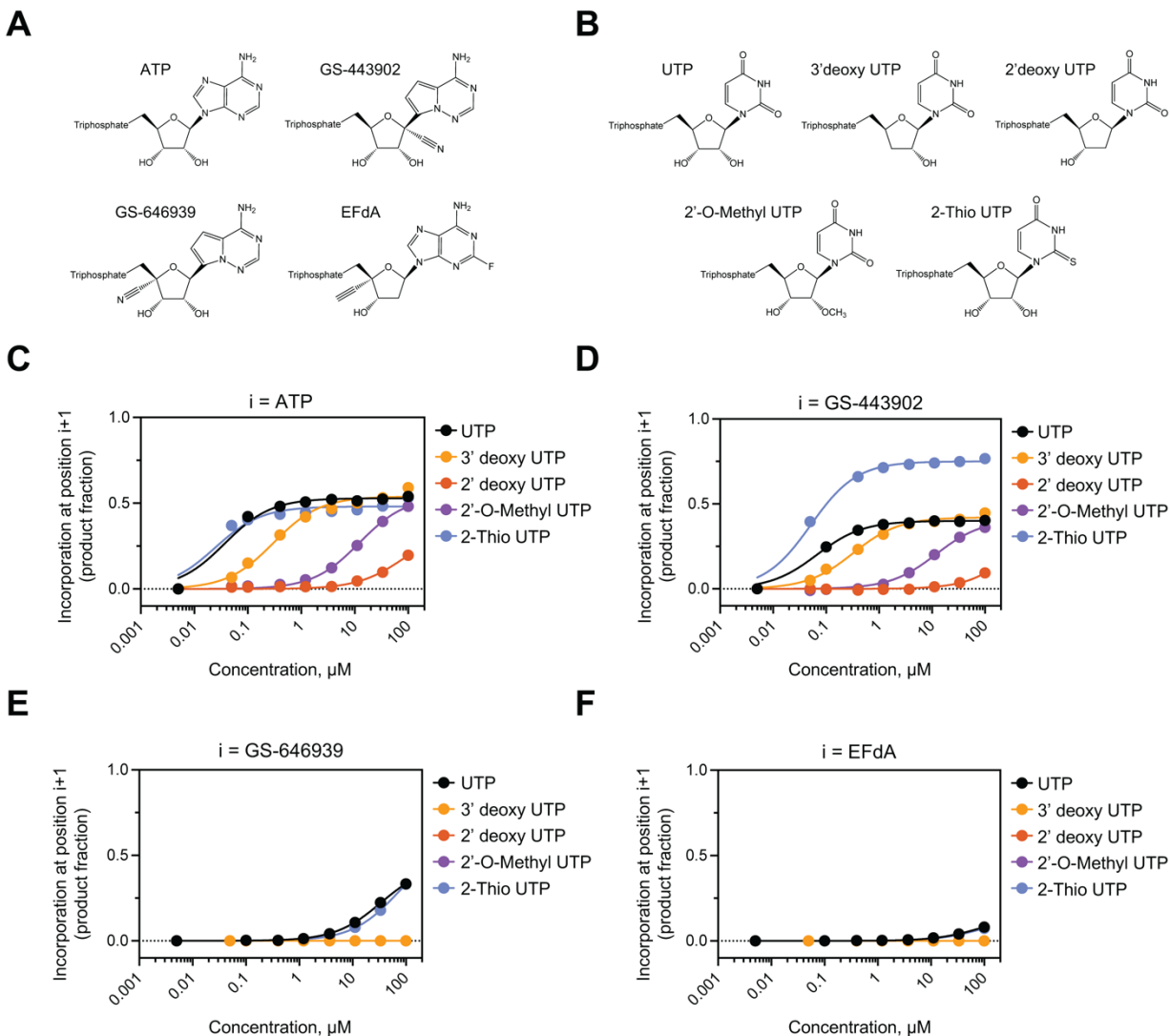


Figure S7. GS-646939 inhibits subsequent nucleotide incorporation catalyzed by HRV-16 RdRp in a manner resembling EFdA. **A**, chemical structures of ATP and ATP analogs. **B**, Chemical structures of UTP and UTP analogs. UTP and UTP analog incorporation at position “ $i+1$ ” was examined at increasing concentrations immediately following incorporation of ATP (**C**), GS-443902 (**D**), GS-646939 (**E**), or EFdA (**F**) at position “ i ”. Product fraction was calculated as the signal generated beyond position “ i ” divided by the total signal in the lane.

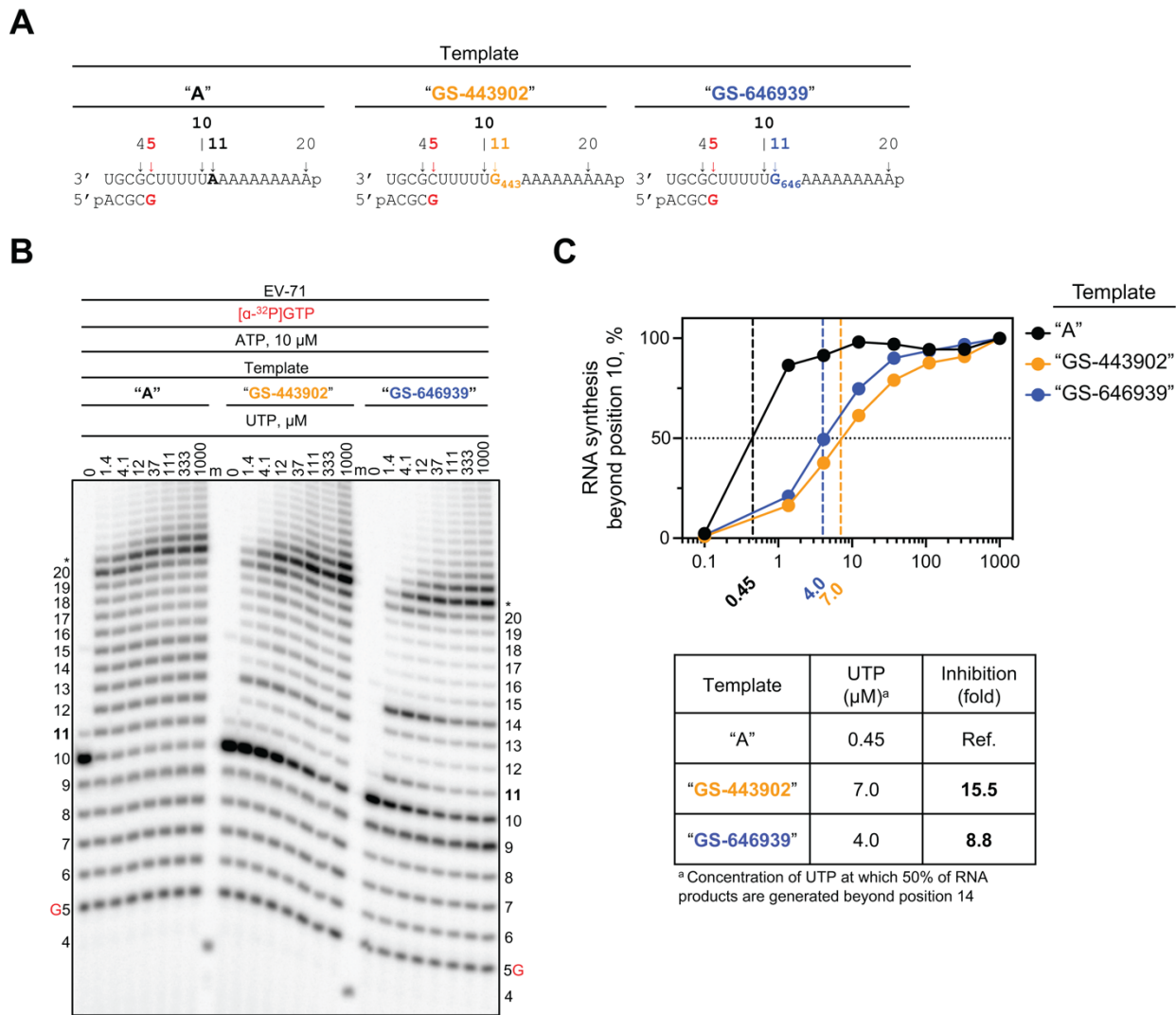


Figure S8. RNA synthesis catalyzed by EV-71 RdRp using a template with a single GS-443902 or GS-646939 residue in the template at position 11. **A**, RNA primer/template with a template-embedded GS-443902 (*Template "GS-443902"*, middle) or GS-646939 (*Template "GS-646939"*, right) at position 11; the corresponding primer/template with adenosine (*Template "A"*) at this position is shown on the left. G5 indicates incorporation of [α -³²P]-GTP at position 5. **B**, Migration pattern of the products of RNA synthesis catalyzed by EV-71 RdRp. MgCl₂, [α -³²P]-GTP, and ATP were provided to the reaction to support RNA synthesis up to position 10. Increasing concentrations of UTP were supplemented to the reactions to monitor incorporation opposite adenosine, GS-443902, or GS646939 at position 11, and templated adenosines from position 12 to 20. For Template "GS-443902", intermediate products are observed at position 10. For Template "GS-646939", additional sites of inhibition are indicated by the formation of intermediate products at positions 9 and 14. Product formation at and beyond the asterisk indicates RNA products that are likely a result of sequence-dependent slippage events. A 5'-³²P-labeled 4-nt primer serves as a size marker **C**, Quantification of **B** (*top*) where the sum of RNA products generated beyond position 10 was divided by the total signal in the lane and normalized as a percentage, fold-inhibition resulting from a templated GS-443902 and GS-646939 (*bottom*). To account for template-dependent differences in activity, product fraction was normalized as a percentage to the product fraction observed at 1000 μ M UTP for that template.

1. Gordon, C. J., Lee, H. W., Tchesnokov, E. P., Perry, J. K., Feng, J. Y., Bilello, J. P., Porter, D. P., and Gotte, M. (2022) Efficient incorporation and template-dependent polymerase inhibition are major determinants for the broad-spectrum antiviral activity of remdesivir. *J Biol Chem* **298**, 101529
2. Tchesnokov, E. P., Feng, J. Y., Porter, D. P., and Gotte, M. (2019) Mechanism of Inhibition of Ebola Virus RNA-Dependent RNA Polymerase by Remdesivir. *Viruses* **11**